An electron-diffraction study of a microcrystalline muscovite and its vermiculitized products[1]

H. KODAMA

Soil Research Institute, Research Branch,[2] Agriculture Canada,
Ottawa, Ontario, Canada

SUMMARY. After approximately 50 % of K from the 1-2 μm fraction of a naturally occurring microcrystalline muscovite was extracted with $BaCl_2$ solution at 98 °C, electron-diffraction patterns showed a honeycomb-shaped diffuse scattering as well as intense diffuse streaks. The diffuse scattering became pronounced with increasing K-depletion. It may be interpreted in terms of a short-range order distribution of interlayer Ba ions, using an analogy to the work by Alcover *et al.* (1972, 1976). Since the diffuse streaks still remained after re-entry of K to the K-depleted specimen they might be related to structural disturbance, particularly in the basal oxygen arrangements, resulting from the K-extraction. Subsequent conversions of Ba-saturated vermiculitized muscovite into Na-, Mg-, and Ca-forms revealed distinct extra diffraction spots midway between two ordinary diffraction spots. They were broader than the ordinary spots and elongated along the three directions of $[01]^*$, $[11]^*$, and $[\bar{1}1]^*$. The diffraction pattern containing the extra spots was, therefore, interpreted as a composite one made up by superimposing three independent patterns, each of which was composed of ordinary Bragg diffraction spots and extra diffraction maxima elongated in one of the three directions. This situation does not require a superlattice but modified the original face-centred lattice symmetry to a primitive lattice symmetry. However, the presence of a real superlattice should also be possible. The elongation and broadness of the extra diffraction maxima may be related to the orientation and size of coherent domains defined by a certain ordering of interlayer cationic distribution, which took place during the hydration processes including extraction and conversion.

CLAY-SIZE micas may be hydrated by an exchange reaction in which their interlayer potassium is replaced by a cation that is more readily hydrated than potassium (e.g. Rausel-Colom *et al.*, 1965). In a previous study (Kodama and Ross, 1973), we achieved more than 90 % potassium extraction from a clay-size muscovite by several successive treatments with $BaCl_2$ solution at 98 °C over a period of three weeks. This extraction resulted in nearly complete interlayer hydration of the muscovite with Ba ions, consequently, the interlayer became expansible and the altered muscovite behaved like vermiculite. In the course of electron-diffraction examinations of the samples at several stages of the K extraction process, various characteristic diffraction phenomena, including diffuse streaks and superlattice reflections, were observed. Since they appeared to be related to the degree of hydration and interlayer cation distribution, a more detailed electron-diffraction study has been carried out by examining samples prepared by replacing Ba conversion from maximum K-depleted muscovite with various interlayer cations. The results obtained are reported herein.

Experimental

Material and sample preparation. The original material from which K was extracted was the 1-2 μm fraction of a naturally occurring microcrystalline muscovite having the structural formula $(K_{0.84}Na_{0.06})(Al_{1.92}Fe^{3+}_{0.07}Mg_{0.04})(Si_{3.06}Al_{0.94})O_{10}(OH)_2$ (Kodama and Brydon, 1968). The fluorine content was negligible, equivalent to only 0.5 % of the total hydroxyls.

Potassium was extracted by treatment with $0 \cdot 1 N$ $BaCl_2$ solution at 98 °C by the procedure described previously (Kodama and Ross, 1973). After three weeks, approximately 93 % of the original potassium was extracted. Intermediate products, which were K-depleted to levels of 26, 56, and 70 %, were similarly prepared by discontinuing the extraction when the amount of potassium extracted reached the required level. The chemical analysis of the 93 % K-depleted sample showed 212 meq Ba and 16 meq K, a total of 228 meq per 100 g sample, which was close to the 226 meq for the original muscovite. Since virtually no loss of charge was observed, it was concluded that the extraction reaction was taking place only in the interlayer of muscovite. The structural formula of the 93 % K-depleted sample may thus be expressed by $(Ba_{0.42}K_{0.06})(Al_{1.92}Fe_{0.07}^{3+}Mg_{0.04})(Si_{3.06}Al_{0.94})O_{10}(OH)_2$ as a dehydrated form will be formed under the high-vacuum condition associated with electron-microscopic observations. The structure and nature of the 93 % K-depleted sample that will hereafter be called Ba-form have been studied and the results indicated a close similarity to those of vermiculite, except for a higher layer charge of the Ba-form (Kodama and Ross, 1973). The Ba-form was subsequently converted into Na-, Mg-, Ca-, Sr-, and Cs-forms by treating with chloride solutions of the respective cations. The specimens saturated with various cations were washed with water until Cl-free and then freeze-dried. An attempt was made to return the Ba-form to the original muscovite by a prolonged treatment with KCl solution at 98 °C for a few weeks. About 98 % exchange of Ba by K was achieved. Based on chemical analysis of these forms, except for the Cs-form where completion of the exchange reaction was questionable, the following interlayer formulae may be deduced:

Na-form: $(Na_{0.80}K_{0.06}Ba_{0.02})$ Ca-form: $(Ca_{0.40}K_{0.06}Ba_{0.02})$
K-form (re-fixed): $(K_{0.88}Ba_{0.01})$ Sr-form: $(Sr_{0.38}K_{0.06}Ba_{0.04})$.
Mg-form: $(Mg_{0.38}K_{0.06}Ba_{0.04})$
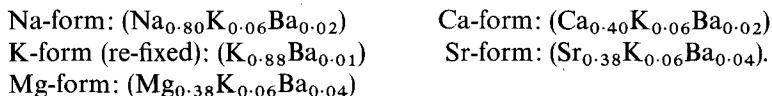
As indicated by the structural formulae, approximately 2 to 10 % of the pre-adsorbed Ba atoms still remained unexchanged after the conversion. Since Ba is divalent with an ionic radius of $1 \cdot 34$ Å, which is very close to $1 \cdot 33$ Å for that of the K ion, it may be considered that Ba ions fit well in the hexagonal cavities of the silicate layers with a strong ionic affinity, and this situation may have caused the difficulty in a complete conversion of the Ba-form into other forms.

Analytical techniques. An approximately $0 \cdot 01 \sim 0 \cdot 02$ % (w/w) suspension of each freeze-dried sample was prepared with the aid of a Vortex Genie mixer after a drop of formaldehyde was added to prevent any possible contamination due to biological activity. Specimens for electron-microscopic observations were prepared by spotting the suspensions on to copper grids coated with thin films of carbon and allowing them to dry at room temperature. The specimens were examined in a Philips EM300 electron microscope with and without a rotation-tilt goniometric specimen stage operating at 80 kV ($\lambda = 0 \cdot 0425$ Å). In one phase of the study, a microphoto densitometer was used to record line profiles of certain microdiffraction spots.

Results and discussion

Diffuse streaks and honeycomb-shaped diffuse scatterings. Fig. 1a and b represent the diffraction patterns of original microcrystalline muscovite and 93 % K-depleted specimen, respectively. Besides the normal hexagonal net pattern, fig. 1b also shows diffuse streaks between ordinary Bragg diffraction spots in the three directions of $[01]^*$, $[11]^*$, and $[\bar{1}1]^*$. Relatively more intense streaks often appeared around reciprocal nodes, 26, $\bar{2}6$, 40, and $\bar{4}0$. The distinction between 26 or $\bar{2}6$ and 40 or $\bar{4}0$ was tentatively made based upon the relationship of the crystal morphology of particles and their diffraction patterns. Although the diffuse streaks are not evident in fig. 1a,
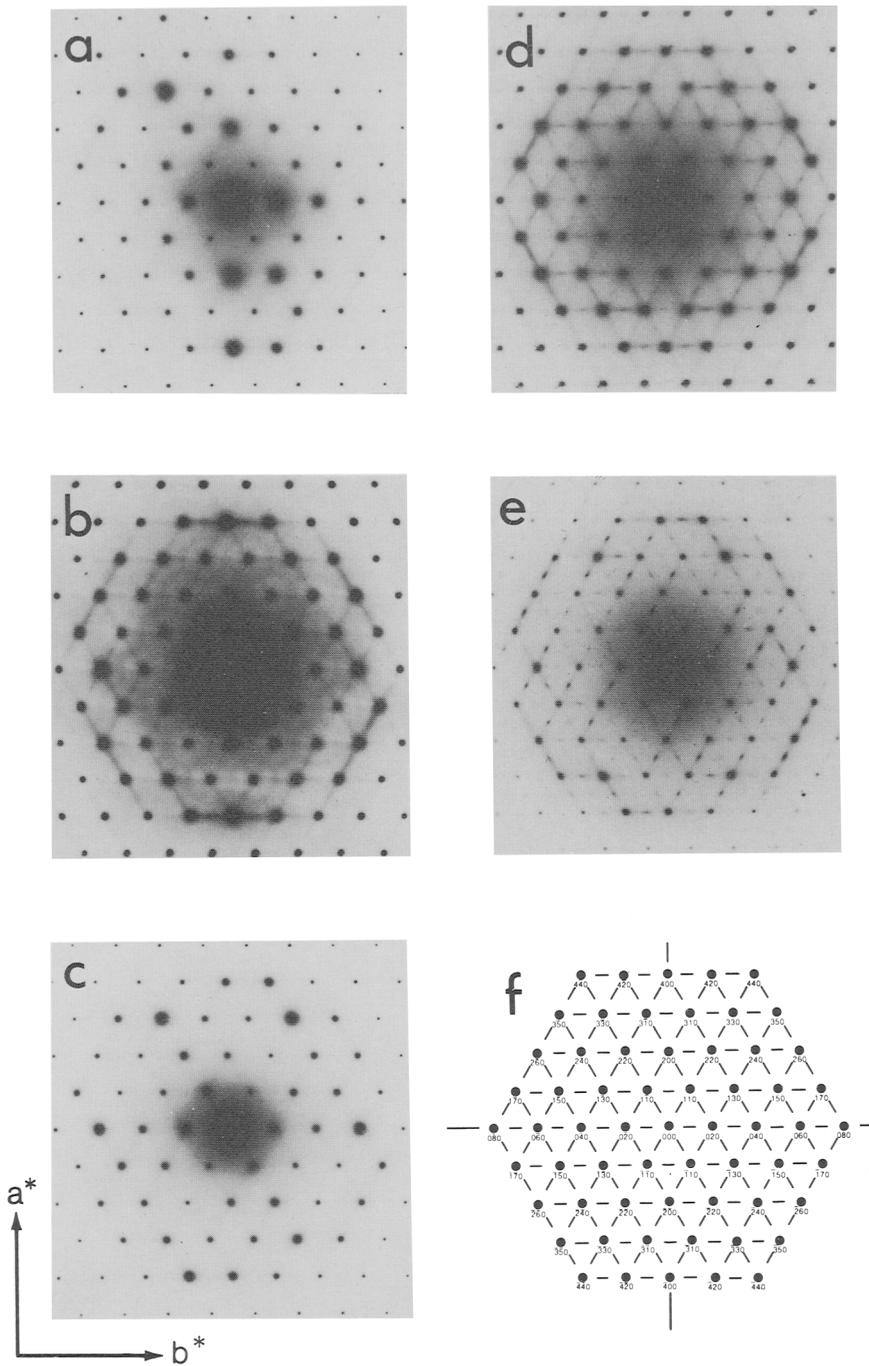
FIG. 1. Electron diffraction patterns of microcrystalline muscovite and its vermiculitized products. *a*—original; *b*—93% K-depleted (Ba-form); *c*—K-form (re-fixed); *d*—Na-form; *e*—Ca-form; *f*—schematic diagram of the diffraction pattern giving indices of reflections.

its negative plate showed weak diffuse streaks. Similar diffuse streaks have also been observed in diffraction patterns (with monochromatic X-rays) of muscovite (Gatineau, 1964), pyrophyllite and talc (Kodama *et al.*, 1971), and in electron-diffraction patterns of pyrophyllite and talc (Kodama, 1975), phlogopite, vermiculite, and saponite (Kodama, unpublished data), and beidellite (Gatineau *et al.*, 1972; Besson *et al.*, 1974; Güven and Pease, 1975). The appearance of such diffuse streaks may be related to certain structural disorders, since pronounced diffuse streaks have been observed in the K-depleted muscovite (fig. 1b) and a dehydroxylated microcrystalline muscovite (Kodama, unpublished data) where certain structural disturbances are likely to be induced during the respective alteration processes.

The diffuse streaks were still observed when crystal particles were tilted around the b^*-axis. Therefore, the diffuse streaks spread along the c^*-axis to constitute plane distributions of the diffuse scatterings, whose directions were parallel to $[010]^*$, $[110]^*$, and $[\bar{1}10]^*$. This should imply the presence of certain monodimensional disorders in crystals along directions perpendicular to the diffuse intensity distributions, i.e. $[100]$, $[\bar{1}10]$, and $[110]$, which coincide with three principal vectors between nearest neighbouring interlayer cations in mica or zig-zag chains formed by joining non-equivalent tetrahedral positions of Si or Al atoms, as seen in fig. 2.

[010]

[$\bar{1}$10]　　　[110]

[$\bar{3}$10]　　　[310]

[100]

OXYGEN [BASAL]　　OXYGEN [APICAL]　　POTASSIUM　　SILICON OR ALUMINUM [PARTLY]
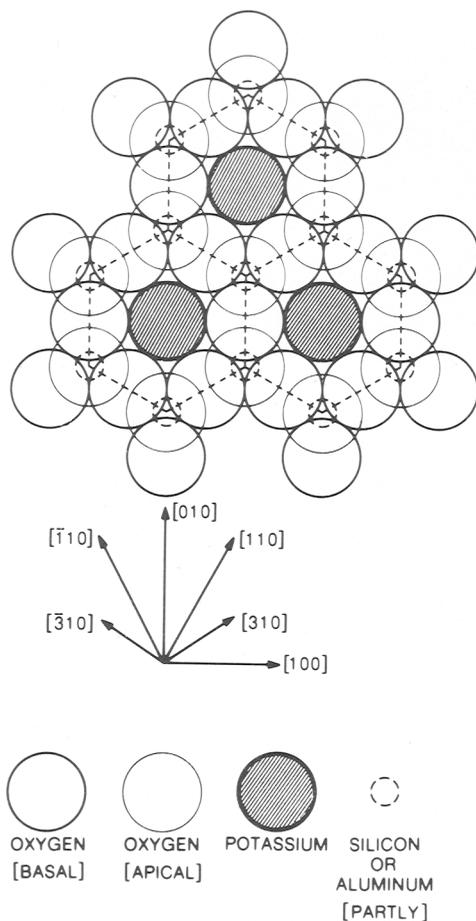
FIG. 2. Schematic diagram of atomic arrangement at the cleavage plane of an idealized muscovite structure.

One cannot, however, conclude that the diffuse streaks are caused by only these atomic arrangements, since pyrophyllite and talc, where neither interlayer cations nor Si–Al substitutions are present, also showed similar diffuse streaks. Therefore, crystal imperfections such as small displacements of atoms, especially oxygens, due to distortion should be taken into account as well as thermal vibrations of atoms.

In addition to the diffuse streaks, another type of diffuse scatterings appeared in the K-depleted muscovite (fig. 1b). The diffuse scatterings are honeycomb-shaped and already became evident after approximately 50% of the interlayer K was extracted. These are considered to consist of short diffuse scattering segments with a length of $2a^*/3$ in three directions of $[10]^*$, $[13]^*$, and $[\bar{1}3]^*$. Since further examinations failed to reveal them in Ba-saturated vermiculite, saponite, and K-depleted phlogopite (Kodama, unpublished data), the honeycomb-shaped diffuse scatterings appear to be unique in the Ba-form of vermiculitized muscovite. The present findings are contrary to those by *in vacuo* X-ray diffraction analysis of Ba-saturated vermiculite crystals, in which a similar honeycomb-shaped diffuse scattering pattern was observed (Alcover *et al.*, 1976). They interpreted the diffuse scatterings in terms of a monodimensional short-range ordering of interlayer Ba ions in the three directions of $[01]$, $[31]$, and $[\bar{3}1]$, which correspond to the principal vectors between second nearest neighbouring inter-layer cations (fig. 2). Because of the incompatible findings mentioned above, the cause of honeycomb-shaped diffuse scatterings cannot be related simply to the presence of interlayer Ba ions.

Diffraction patterns after conversion into other forms. The replacement of Ba ions by K or Cs ions produced diffraction patterns similar to that of original muscovite (cf. fig. 1a and c). When the Ba-form was converted into Na-, Mg-, and Ca-forms, superlattice reflections appeared instead of honeycomb-shaped diffuse scatterings (fig. 1d and e). Due to weak intensities of the reflections, the presence of the superlattice reflections had to be confirmed by examination of *diffraction photographs taken with a rather long exposure time. Observations on many separate particles of the Na-, Mg-, and Ca-forms indicated that the frequency for the appearance of superlattice reflections was approximately two-thirds (or 67%) of the total observations, regardless of interlayer elemental species. In the rest of observations (one-third), the superlattice reflections were replaced by diffuse streaks, which differed from those observed previously in that the intensities peaked midway between ordinary diffraction spots. The effect was less obvious for the Sr- and Ba-forms. Such diffuse streaks or superlattice reflections were not noted in X-ray diffraction observations by Alcover *et al.* (1972) on dehydrated Ni- and Mg-vermiculite crystals.

To determine whether the superlattice reflections were real or due to double diffraction effects, crystal particles as thick as possible were chosen and tilted about the b^*-axis or pseudo-b^* axis containing the superlattice reflections. Since the superlattice reflections did not disappear, they must be real. If the superlattice reflections are round spots like ordinary diffraction spots, their appearance could then mean the presence of a two-dimensional superlattice whose lateral dimensions are twice as large as those of the original muscovite ($a = 5\cdot2$, $b = 9\cdot0$ Å). In most cases, however, the superlattice reflections were elongated in three directions parallel to $[01]^*$, $[11]^*$, and $[\bar{1}1]$ (fig. 1d and e). Therefore, the reflections can be grouped by the three respective directions in which they were elongated and those belonging to one group can be treated independently of others (fig. 3). The diagram of diffraction pattern containing superlattice reflections elongated in the direction parallel to $[01]^*$ is shown in fig. 3a. Rotating the diagram 60° and 120° around the c-axis yields the other two diagrams (fig. 3b and c) corresponding to those of diffraction patterns containing superlattice reflections elongated in directions parallel to $[11]^*$ and $[\bar{1}1]^*$, respectively.
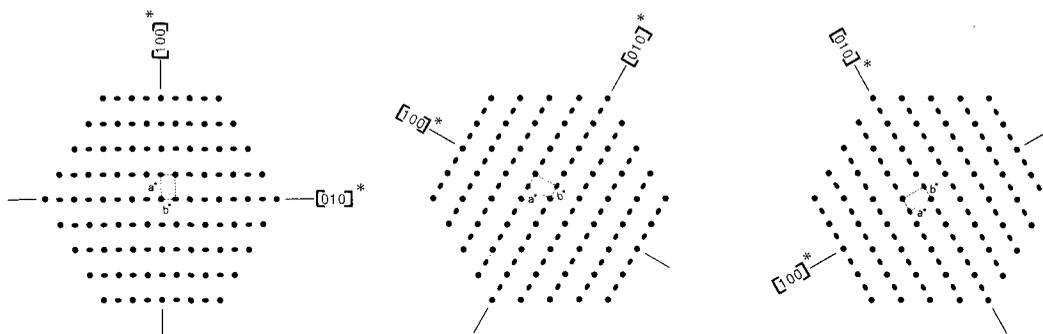
FIG. 3. Schematic representation of three principal orientations of the electron-diffraction patterns containing extra reflections.

Original unit-cell dimensions remained unchanged as outlined by the dotted line in fig. 3 but the symmetry was changed from face-centred to primitive. Thus, the electron-diffraction patterns containing superlattice reflections as represented by fig. 1f may be interpreted as a result of superimposition of the above three independent patterns. This implies that within one crystallite, the orientation of crystal symmetry in a certain layer or layers differs from that in an adjacent layer or layers.

The degree of elongation or broadness of the superlattice reflections is related to a coherent domain size defined by the extension of a certain structural ordering. The domain size may be evaluated by treating the diffraction broadening as in the case of X-ray diffraction (Klug and Alexander, 1954) using the equation with approximation: $D \approx \lambda/(\beta\cos\theta) \approx \lambda/\beta$ (since $\theta \doteq 0$), where λ is the wave length of electron beam and β is the half-maximum breadth of the reflection in radians. The β's were determined from microphotodensitometric traces along the direction of elongation of superlattice reflections. The results indicated average dimensions ranging from 45 to 95 Å. Thus, a group of the superlattice reflections elongated in the direction parallel to $[01]^*$ implies that in a crystal the domain defined by a structural ordering along the $[10]$ direction is terminated with a periodicity of around 45 to 90 Å. Similarly, for those elongated along $[11]^*$ and $[\bar{1}1]^*$ directions, the corresponding directions are $[\bar{1}1]$ and $[11]$, respectively. The appearance of such superlattice reflections may be explained by a partial ordering of interlayer cations as discussed in the next section.

An interpretation of the occurrence of superlattice reflections. As mentioned in the preceding section, the extra diffraction maxima elongated along the three directions of $[01]^*$, $[11]^*$, and $[\bar{1}1]^*$ may also be interpreted as a composite one made up by superimposing three independent patterns, each of which is composed of ordinary diffraction spots and the extra diffraction maxima elongated along one of the three directions. Each component pattern has nearly the same cell parameters along the a and b axes as those of the original muscovite but its face-centred lattice symmetry is modified to a primitive one. In a crystal particle, thus, it may be considered that layers having the primitive lattice symmetry are randomly stacked together with a relative orientation of $\pm n \times 60°$.

The most plausible reason for the occurrence of extra diffraction maxima may be interlayer cation distribution. Fig. 4a represents a schematic diagram of interlayer K-ion distribution in muscovite having a and b cell dimensions with the face-centred lattice symmetry. When the K ions are replaced, hydrated interlayer cations redistribute themselves. Subsequent dehydration causes interlayer cations to migrate into hexagonal cavities vacated by the original K ions. For

simplicity, let us take an example consisting of monovalent interlayer cations only, e.g. Na ions and the remaining K ions. Fig. 4b shows an ideal distribution among Na and K ions (in the case that Na > K) that constitutes a superlattice with cell dimensions, $a' = 2a$ and $b' = 2b$, while its lattice symmetry is maintained as face-centred. This type of distribution is fulfilled by the K ions occupying the interlayer sites marked with solid circles, which are located at a centre and corners of the superlattice outlined by the dotted line. These correspond to two out of eight sites available for a unit superlattice. Thus, the ratio of K to Na ions for the ideal distribution should be one-third (= 0·33). Although there was no clear evidence for this type of distribution, because of the suspected superimposition the possibility of superlattice in certain layers cannot be ruled
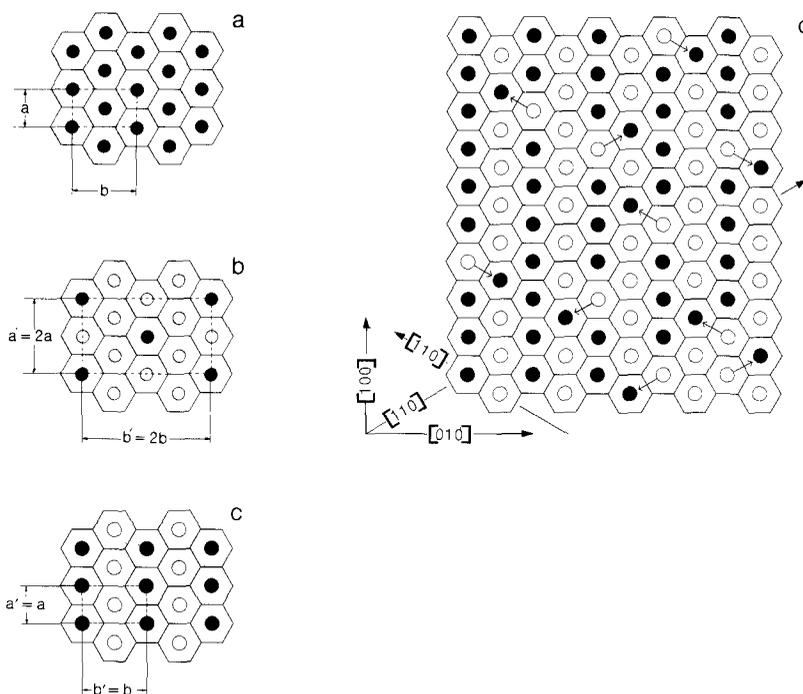
FIG. 4. Schematic representations of interlayer cation distribution. a—inter-layer K atoms in muscovite with a face-centred cell; b—ideal distribution of interlayer cations (K atoms and atoms of another kind) constituting a superlattice structure; c—ideal distribution of interlayer cations (the two kinds) constituting a primitive cell; d—alternating sequence of atoms of the two kinds (as c) along [010] direction with probable 'out-of-steps' of atoms from the ideal atom rows. (Only four directions are indicated by arrows.)

out. Fig. 4c represents an ideal distribution that satisfies the primitive lattice symmetry without changing the original cell parameters of muscovite. In this case, the ratio of K to Na ions becomes 1:1 (= 1·00). The ratio may, therefore, be a determining factor for the choice of lattice symmetry. In either case, with the ratio of 0·33 or 1·0, there will be three possible directions parallel to [10], [11], and [$\bar{1}$1] for the orientation of the K–Na substitution arrays and the direction of alternating sequence of the K and Na atom arrays. The extension of such regular distributions will be terminated by 'out-of-steps' of the atoms from their regular sites, which may occur in six possible directions parallel to [10], [11], and [$\bar{1}$1] (fig. 4d). Thus, the three principal directions are also related to the size and elongation of domains that were determined by the way in which the 'out-of-steps' occurred. Actual cases are obviously made more complex by the

presence of divalent cations including a small number of remaining Ba ions, and the consequent vacancy of some sites. Furthermore, electron-microscope microprobe analyses (EMMA; Jepson and Rowse, 1974) of thirty separate particles of a similar material (Ca-form) indicated that there were some significant variations in interlayer cation concentrations from particle to particle, suggesting that many variations in interlayer cation distribution might be expected in a sample.

Because of this, the hypotheses proposed were not examined quantitatively at the present stage. Since the distribution ordering should depend upon how well the interlayer is hydrated to redistribute interlayer cations before dehydration brings them into the hexagonal cavities, the question remains whether the redistribution is controlled by the interlayer cations themselves or influenced by a negative charge distribution pattern determined by ionic substitution in the silicate layers of the original muscovite.

REFERENCES

Alcover (J. F.), Gatineau (L.), and Méring (J.), 1972. *Clay and Clay Miner.* **21**, 131–6.
———————and Kodama (H.), 1976. Ibid. (in press).
Besson (G.), Tchoubar (C.), and Méring (J.), 1974. *J. Appl. Cryst.* **7**, 345–50.
Gatineau (L.), 1964. *Bull Soc. fr. Minéral. Cristallogr.* **87**, 321–55.
——Tchoubar (C.) and Méring (J.), 1972. Ibid. **95**, 713–21.
Güven (N.) and Pease (R. W.), 1975. *Clay Miner.* **10**, 427–35.
Jepson (W. B.) and Rowse (J. B.), 1974. *Clay Minerals Soc., Ann. Meet. Prog.,* 39. October 1974, Cleveland, Ohio, U.S.A.
Klug (H. P.) and Alexander (L. E.), 1954. *X-ray diffraction procedures for polycrystalline and amorphous materials.* Ch. 9, 491. John Wiley & Sons, Inc. (New York).
Kodama (H.), 1975. In *Contributions to Clay Mineralogy,* in honour of Professor Toshio Sudo, 7–13.
——Alcover (J. F.), Gatineau (L.), and Méring (J.), 1971. In Symposium *Structure and Surface Properties of Clay Minerals,* Louvain, Belgium (abstract).
——and Brydon (J. E.), 1968. *Trans Faraday Soc.* **64**, 3112–19.
——and Ross (G. J.), 1973. *Proc. 1972 Int. Clay Conf.* Madrid, 481–92.
Rausel-Colom (J. A.), Sweatman (I. R.), Wells (C. B.), and Norrish (K.), 1965. *Studies in the artificial weathering of mica* in *Experimental Pedology,* 40–70 Butterworth, London.